Large-scale auralised sound localisation experiment

Enzo De Sena[1], Neofytos Kaplanis[2,3], Patrick A. Naylor[4], and Toon van Waterschoot[1,5]

[1]*KU Leuven, ESAT–STADIUS, Stadius Center for Dynamical Systems, Signal Processing and Data Analytics, Kasteelpark Arenberg 10, 3001 Leuven, Belgium*

[2]*Bang & Olufsen, Peter Bangs Vej, 15, 7600 Struer, Denmark*

[3]*Department of Electronic Systems, Aalborg University, 9220 Aalborg, Denmark*

[4]*Department of Electrical and Electronic Engineering, Imperial College, London SW7 2AZ, United Kingdom*

[5]*KU Leuven, ESAT–ETC, Advise Lab, Kleinhoefstraat 4, 2440 Geel, Belgium*

Correspondence should be addressed to Enzo De Sena (`enzo.desena@esat.kuleuven.be`)

ABSTRACT

Nearly nine hundred people participated in a binaural sound localisation experiment during a science exhibition. The aim of the experiment was to investigate subjects' localisation performance in an informal setting and with little training, which, in comparison to formal listening experiments, are conditions more similar to those encountered in consumer applications of binaural audio. The subjects wore headphones while standing on a rotating platform. Their task was to rotate the platform until a sound source auralised through the headphones was perceived to be in front of them. The test was carried out using different head related transfer function (HRTF) datasets, programme material, and virtual acoustical conditions. An analysis of the data shows that (a) more than half of the subjects could localise the sound source with less than 7.5 degrees of error, (b) twelve percent of the subjects experienced a front/back reversal, (c) by selecting measured HRTFs randomly from one of two datasets, the KEMAR measurement resulted in a larger localisation error than the chosen measurement from the CIPIC database.

1. INTRODUCTION

The localisation of sound sources on the horizontal plane is mostly reliant on binaural cues and, more specifically, on the differences in level and time shift between the ears [1]. Interaural level differences (ILDs) are caused by the acoustical shadowing of the head and are strongly frequency-dependent. Interaural time differences (ITDs) are caused by the different time of arrival of sound waves at the two ears. At low frequencies the auditory system analyses the interaural time shifts between the signals' fine structure [1]. At higher frequencies this mechanism becomes ambiguous, and the time shift between signals' envelopes is used instead [1, 2].

The ILD and ITD cues are often not sufficient for localising sound sources in the three dimensions. In fact, there is a whole locus of points, usually called "cone of confusion", with similar ILD and ITD cues [1]. Humans tend to solve the front/back ambiguity by means of more



Fig. 1: The rotating platform used for the experiment.

or less unconscious head movements [2]. Additionally, the auditory system exploits the strong dependence of the head related transfer function (HRTF) on the source elevation [1].

In this experiment, the perceptual cues that are experienced in natural hearing are reproduced through binaural rendering in headphones by filtering with chosen HRTFs obtained from datasets of HRTF measurements. The azimuthal head position is monitored in real-time and the rendering is updated dynamically to reflect head orientation changes, which is necessary to achieve sound externalisation and to reduce the likelihood of experiencing front/back reversals [3].

A large number of experiments have been carried out in the past to study sound localisation on the horizontal plane. Early experiments, some of which date back to the 1920s, focused on the so-called localisation blur, i.e. the smallest change in a given attribute that is sufficient to change the perceived location of the sound source [1]. Others investigated persistence, adaptation and learning effects, and the influence of the source's spectral content and its movement [1]. Various experiments studied the localisation of isolated sound sources in rooms [1, 4] or of multiple sound sources in free field [1, 5]. Most of these experiments relied on a relatively small number of trained subjects. The aim of this experiment, on the other hand, was to investigate subjects' localisation accuracy in an informal setting and with little training, which are conditions that are closer to those encountered in typical consumer applications of binaural audio.

This paper is organised as follows. Section 2 describes the experimental method in detail. Section 3 presents the data analysis. Section 4 concludes the paper.

2. METHOD

2.1. Participants

The subjects of the experiment (N=893) were visitors of the Royal Society Summer Science Exhibition, which was held in London in early July 2015. Entry to the exhibition was free of charge. Most visitors were science aficionados, families and school pupils.

All subjects were informed that their performance in the localisation task would be recorded. No information of individual subjects was collected. Their age ranged from 10 to 70 years old and no gender bias was observed.

2.1.1. Data Monitoring

At least one experimenter was present at all times. The following anomalies were observed. Two subjects declared they were deaf in one ear and their performance was removed from the data. The performance of another 38 subjects was removed for one of the following reasons: (a) the subject declared after the experiment that he/she did not actually understand the task, (b) the subject declared after the experiment that he/she made a mistake in using the interface, or (c) the subject was of very young age and appeared to be playing with the rotating platform rather than concentrating on the given task.

Since the experiment was self-controlled, each subject could run the test multiple times. In case a subject performed the task under the exact same conditions more than once, the additional data points were excluded in order to avoid biases due to learning effects. Twenty-seven data points were also excluded because one of the experimenters was not aware that the interface had to be reset every time a new subject joined the experiment, which resulted in non-counterbalanced variable control. In addition, twenty-two tests were removed because the subject gave a response in less than one second, indicating that he/she touched the interface two times in quick succession by mistake.

The above post-processing reduced the number of subjects from 893 to 844, and the total number of data points from 1979 to 1655.

2.2. Apparatus

The subject stood on the rotating platform shown in Fig. 1. They could freely turn themselves around a stationary wheel in the centre of the rotating platform. The subject wore a pair of Bang & Olufsen BeoPlay H6 headphones connected to the iPad Air. The iPad showed the graphical user interface (GUI) and was mounted in front of them at eye level. The iPad could be shifted up and down to adjust for the subjects' eye-height. During the experiment, the physical movement was tracked in real-time and the user interface provided a visual feedback to the subject, as shown in Fig.2c.

The rotation angle of the platform was measured by means of the iPad's motion sensor. This motion sensor was found to be sufficiently stable and precise for the purpose of this experiment, which was verified as follows. Leaving the iPad lying on a stable surface for 1 minute and repeating this ten times yields an average maximum drift of 0.67 degrees. Turning the iPad ten

times around itself gives an average deviation from the expected 180 degrees of about 2 degrees.

2.3. Procedure

The experimenter introduced the subject to the apparatus and the task. The subject could then run the experiment, in a self-paced and self-controlled manner. A custom GUI, depicted in Fig.2, enabled subjects to control the experiment. They could choose to run the experiment under two conditions–an anechoic condition and a reverberant condition[1]. The details of the sound stimuli in the two cases are explained in detail in the next subsection. The subjects could run the different cases in any desired order and any number of times. Most subjects ran the anechoic case once, and the reverberant case, also once.

The subjects were instructed to stay as still as possible and to keep looking at the iPad for the entire duration of the experiment. Based on the assumption that the subjects' head would rotate in unison with the rotating platform, the iPad was used as a head tracker. The HRTFs filters were dynamically updated based on the current position of the head.

Once the test started, the subjects' task was to rotate the platform until the sound source appeared to be in front of them. The audio sample was looped, which allowed the subject to take as much time as needed.

Once finished, they touched the iPad to record their decision. At this point the GUI would show their performance in terms of angular error. The interface would show a congratulation message in case the angular error was below ± 20 degrees. In case the angular error was above ± 170 degrees, the interface would inform the subject that he/she experienced a front/back reversal.

Neither the subject nor the experimenter were aware of the true angle of the sound source until after the end of the test. In cases where a queue would form, the subjects could see others taking the experiment before them.

2.4. Sound stimuli

2.4.1. Programme material

Two anechoic sound samples from the "Music for Archimedes" CD [6] were used: (1) the female speech sample (track number 4), and (2) the african percussions sample (track number 26). The samples were in waveform audio file (WAV) format. In order to reduce memory spooling, the two samples were shortened to 28 seconds and 25 seconds, respectively.

According to the ISO-523 model [7], the percussions sample was 4.4 dB louder than the speech sample[2]. The same samples were also evaluated using the loudness model for time-varying signals proposed by Glasberg and Moore in [8], which gave an opposite result, with the speech sample being 4 sones louder than the percussion sample on average. The two stimuli were confirmed by human ear to have a perceptually similar loudness.

2.4.2. Head related transfer function (HRTF)

The anechoic sample was filtered through one of two HRTF datasets: the MIT measurement of the KEMAR mannequin [9], and one of the measurements of a human subject in the CIPIC database [10]. One of the two datasets was selected at random for each new subject. The initial look direction with respect to the position of the sound source was randomised with uniform distribution for each new test. The two HRTF datasets were equalised such that the energy of the response in the frontal direction was identical.

The CIPIC database consists of high-resolution HRTFs measured at the entrance of the ear canals of 43 subjects. Along with the two ear signals, the database also contains measurements of a number of anthropometric features (e.g. head width, ear height etc) for each subject. The particular subject used in this experiment was the one with the anthropometric features closest to the average of the CIPIC database. This was calculated by ranking each anthropometric feature according to the distance from the mean of that feature. The one with the highest average ranking was then chosen. According to this procedure, the subject closest to the anthropometric average was number 58.

The horizontal resolution for frontal directions was 5 degrees for both datasets. The spatial sampling outside the horizontal plane (used during room simulations) differed between the two datasets (for details, see [9] and [10]). In order to avoid spatial aliasing issues associated to HRTF interpolation and due to informal nature of the experiment, switching on the 5-degrees azimuth grid was considered sufficient. Platform rotation did not cause audible clicks.

[1] A third case with a sound source and an echo was also included, but results are not reported in this paper.

[2] The speech sample was reduced by 3dB with respect to the level of the CD track.

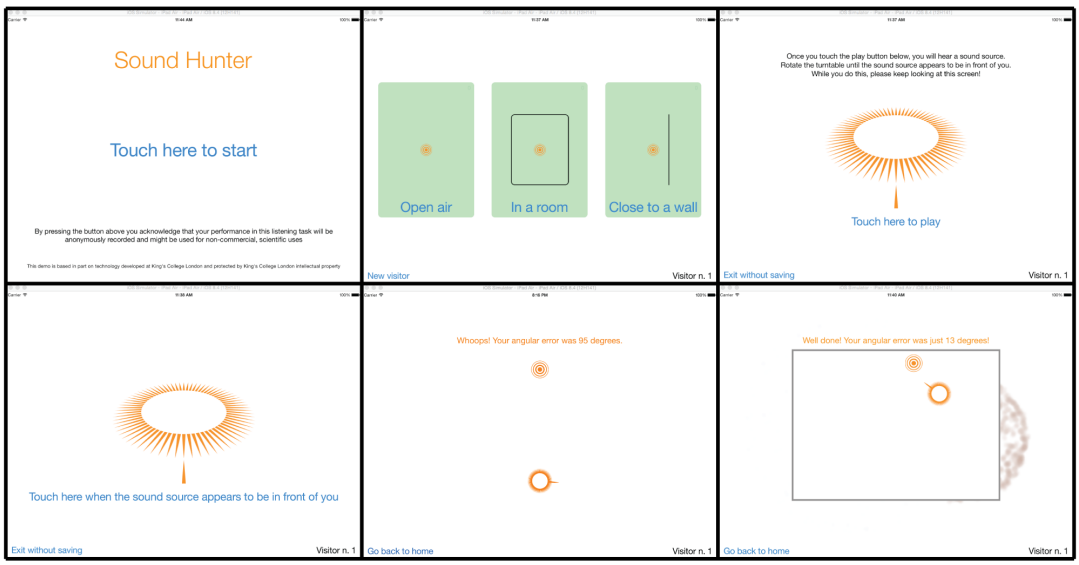

Fig. 2: Overview of the GUI. From top-left, reading left to right, to bottom-right: (a) splash screen with disclaimer, (b) selection of type of simulation, (c) instructions on how to run the experiment (the same information was repeated by the experimenter), (d) interface with a 3D compass rotating according to the movement of the platform, (e) example of test outcome in case of anechoic condition and perceived direction far to actual direction, and (f) example of test outcome in case of reverberant condition and perceived direction close to actual direction.

2.4.3. Anechoic condition

In the anechoic condition, subjects had to localise a sound source that was positioned at the same height as the listener.

2.4.4. Reverberant condition

In the reverberant condition, the room acoustic response was simulated using a scattering delay network (SDN) [11]. Among the many available room acoustic models, SDN was chosen because it is capable of running in real-time while also reproducing faithfully important physical and perceptual features. An SDN, which is shown conceptually in Fig. 3, is a a delay-network-based model. As opposed to typical models in this class, SDN is capable of simulating the acoustics of a room with specific physical characteristics, e.g. room size, wall absorption etc.

Due to its design, SDN renders the line-of-sight component and first-order reflections exactly (both in time, amplitude, as well as HRTF weighting), while making progressively coarser approximations of higher-order reflections. In addition, due to the way energy losses are implemented in the network (see [11] for details), and to the fact that the mean-free-path of the network is similar to the one in the modelled room, the energy decay rate is close to that obtained in geometric-based models, e.g. the image method (IM) [12]. The time evolution of the normalized echo density (as defined in [13]) is also close to that of the IM. Thus SDN approaches the accuracy of full-scale room simulation while having the computational efficiency of typical methods based on delay networks.

Three different conditions were tested in the reverberant case: (a) typically-sized living room, (b) room with higher ceiling and higher reverberation time, and (c) room with normal ceiling and higher reverberation time. In all cases, the walls had an absorption characteristic that was independent of frequency. The specific room dimensions and wall absorption coefficients for the three cases are shown in Table 1, along with the resulting reverberation time T_{60} and direct-to-reverberant ratio (DRR). The room dimensions of (a) and (c) are compliant with the ITU-R standard [14]. The wall absorption coefficient of case (c) was chosen such that its reverberation time is the same as case (b). In all cases, the listener

Condition	Width L_x	Length L_y	Height L_z	Wall abs. coeff.	T_{60}	DRR
Typical room	7.35 m	5.33 m	2.5 m	0.36	0.30 s	1.0 dB
High ceiling	7.35 m	5.33 m	8.0 m	0.36	0.45 s	4.5 dB
High reverb.	7.35 m	5.33 m	2.5 m	0.30	0.45 s	0.2 dB

Table 1: Characteristics of the room simulation in the reverberant condition.

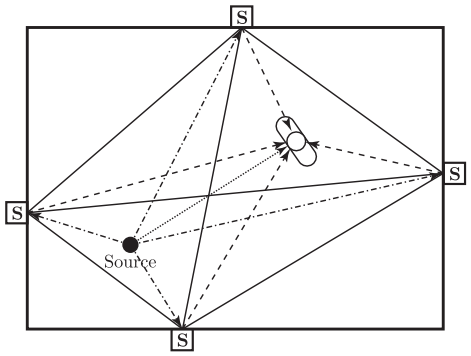

Fig. 3: Conceptual depiction of the SDN method in a 2D rectangular room (the simulations in this paper use a full 3D case). The solid black lines denote bi-directional delay lines interconnecting the wall nodes. The wall nodes are denoted by the **S** blocks. The dash-dotted lines denote mono-directional absorptive delay lines connecting the source to the wall nodes. The dashed lines denote mono-directional absorptive delay lines connecting the wall nodes to the microphone. The dotted line denotes the direct-path component. Adapted from [11].

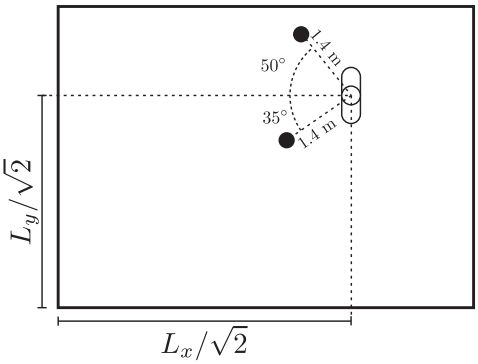

Fig. 4: Setup of the reverberant simulation. The black circles denote the position of the sound sources. Only one source was playing at a time.

was placed at a position $[x,y,z] = \left[L_x/\sqrt{2}, L_y/\sqrt{2}, 1.75\right]$. This setup was chosen to be simple to describe and reproduce, while at the same time not very regular (e.g. the room dimensions being multiple integers of the listener position), which was shown to yield audible artifacts in rectangular geometries [15].

The sound source was positioned in one of two possible positions. Both positions were at a distance of 1.4 m from the listener but at different angles, as shown in Fig. 4. The sound level of the line-of-sight component was the same as in the anechoic condition.

In summary, the experimental design for the reverberant case was based on a $2 \times 2 \times 2 \times 3$ between-subjects design (i.e. two HRTFs, two anechoic audio samples, two source positions and three room types). The subject and the experimenter knew whether the test was a anechoic or a reverberant case, but neither one knew which particular condition was being tested.

2.4.5. Implementation details

The convolutions with the HRTF dataset were implemented via finite impulse response (FIR) filters running in real-time on the iPad. When the look direction changed, the coefficients of the FIR filter were updated. The state of the FIR filter, on the other hand, was left unchanged, which provided a sufficiently smooth transition between look directions. The iPad's motion sensor was polled once every 50 ms.

The frequency response of the headphones was equalised via minimum-phase, inverse filters. The response was measured with a NTI M2210 microphone attached to a closed wood cavity using the exponential sine sweep method.

The software generating the sound stimuli was written

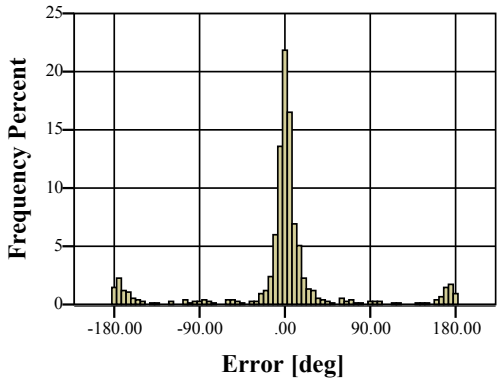

Fig. 5: Histogram of error in the anechoic condition. The resolution of the histogram is 5 degrees, which corresponds to the resolution of the HRTF datasets.

in C++, while the GUI was written in Objective-C. The single-core CPU usage was always below 30% on average, with peaks of about 50%. No buffer underflows or audio glitches were reported.

3. DATA ANALYSIS

The analysed data included responses (N=1655) from the two listening conditions (a) anechoic (N=751) and (b) reverberant (N=904). Before carrying out the following data analysis, the angular data was quantised to the closest 5 degrees. This was motivated by the fact that, even though the iPad motion sensor gave angular readings on a continuous scale, the actual changes in angular perception occurred in discrete steps, due to the finite resolution of the HRTF datasets.

Fig. 5 shows the distribution of the angular error in the anechoic case. Twenty-two percent of subjects made an error smaller than ± 2.5 degrees, i.e. they were capable of identifying the sound source exactly. Fifty-two percent made an error smaller than ± 7.5 degrees. Fifteen percent of the subjects made an error larger than ± 92.5 degrees. Twelve percent made an error larger than ± 152.5 degrees, indicating that they experienced a front/back reversal.

The mean value of the angular error is -2.0 degrees. It should be observed, however, that mean values of a circular quantity like the angular error are not really informative when calculated over the entire ± 180 degrees range. Consider, for instance, a random variable with probability density function (PDF) uniform over angles larger than ± 90 degrees, i.e. directions behind the subject. The mean of this random variable is 0 degrees, while in fact the distribution is centred around the direction directly at the back of the subject, i.e. 180 degrees. One way to overcome this problem is to compute mean values of errors within a limited angular sector around the centre, e.g. $\pm 45^\circ$ or $\pm 20^\circ$ [16, 17]. These errors are often referred to in the literature as *genuine errors* [17]. In this paper, genuine errors are assumed to be those within ± 42.5 degrees. Reversal errors are treated as a special class of error [18, 19].

From the histogram, it is clear that the error distribution is not normally distributed. A Kolmogorov-Smirnov test rejects the hypothesis that the data is normally distributed with $p<0.001$. Also the error distribution between ± 42.5 is not normally distributed ($p<0.001$). For this reason, non-parametric statistical tests, e.g. Mann-Whitney and binomial tests, are used in the remainder of this paper.

Table 2 presents a summary of the statistics of genuine errors. In the anechoic case, the mean is $+1.84$ degrees. A binomial test run on the binary left/right variable reveals that this bias is statistically significant ($p<0.001$). This bias is consistent with the prior art [20, 21], though it cannot be completely ruled out the possibility of small systematic experimental errors due to, for example, asymmetries in the apparatus or in the HRTF datasets.

Surprisingly, the data also indicates that speech yields a stronger rightward bias than percussions. If one considers the genuine errors for both the anechoic case and reverberant case, the percussions sample (N=673) and speech sample (N=676) yield a mean error of $+1.08$ degrees and $+2.57$ degrees, respectively. A Mann-Whitney test (2-tailed) reveals that this small difference is statistically significant (p=0.031).

There is also a small but statistically significant difference between the two HRTF datasets. If one considers the genuine errors for both the anechoic case and reverberant case, the KEMAR mannequin (N=647) and subject 58 of the CIPIC database (N=702) yield a mean error of $+2.36$ degrees and $+1.35$ degrees, respectively. A Mann-Whitney test reveals that the deviation between the two HRTF datasets is statistically significant (p=0.004).

Fig. 6a shows the mean genuine error as a function of the programme sample and acoustical condition. The rightward bias of the speech sample is clear in this figure. Furthermore, a strong bias is observed for the room with higher reverberation time. This can be explained by

Condition	Mean	SD	HRTF	Progr. material	Source position	Front/back reversals
Anechoic	+1.84 deg	10.68 deg	**p=0.050**	p=0.178	-	12.1%
Typical room	+1.52 deg	11.04 deg	p=0.126	p=0.069	p=0.424	10.0%
High ceiling	+1.43 deg	11.27 deg	**p=0.037**	p=0.264	**p=0.039**	10.5%
Higher reverb.	+2.55 deg	11.18 deg	p=0.113	**p=0.030**	**p=0.001***	10.5%
All combined	+1.83 deg	10.94 deg	**p=0.002***	**p=0.015***	**p=0.003***	11.2%

Table 2: Statistics of the genuine errors. Interactions are calculated with the Mann-Whitney test (1-tailed, Monte Carlo), with p-values in boldface indicating statistical significance at the 0.05 level. The asterisk indicates interactions that are also significant with the 2-tailed Mann-Whitney test at the 0.05 level.

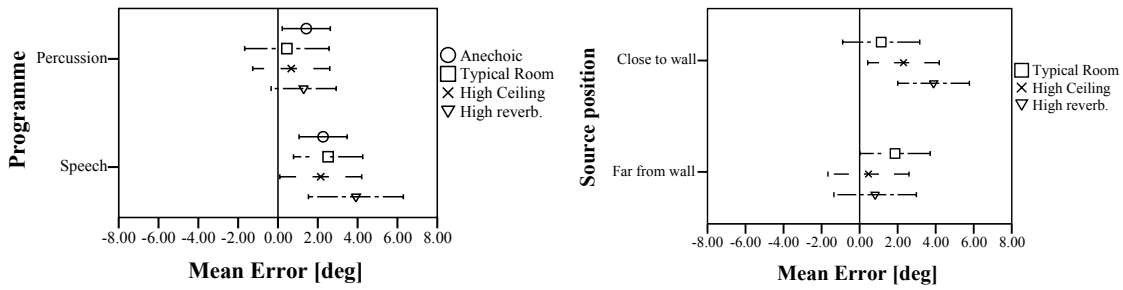

Fig. 6: Mean of the genuine errors for (a) the two programme materials and (b) the two source positions in the reverberant condition. The error bars represent the 95% confidence intervals.

looking at Fig. 6b. Here, it is clear that the sound source closer to the wall has a significant rightward bias compared to the source far from the wall (p=0.003). This is likely to be attributed to a relatively strong first-order reflection positioned to the right of the sound source (see Fig.4). For the case with higher reverberation time, this reflection has a level 5% higher, which leads to a stronger rightward bias.

4. CONCLUSIONS

This paper reported on the design of a sound localisation experiment carried out during the Royal Society Summer Science Exhibition. Nearly nine hundred people participated in the experiment. An analysis of the data showed that more than half of the subjects localised the sound source with an error smaller than 7.5 degrees and that 12% of them experienced a front/back reversal. It also revealed a small but statistically significant rightward bias of a speech audio sample with respect to a percussions audio sample. The MIT measurement of the KEMAR mannequin was also shown to yield a larger error than the measurement of subject 58 in the CIPIC database.

Further work is needed to analyse in detail the vast amount of data that was collected during the experiment. The data is available online at [22].

ACKNOWLEDGMENT

This research work was carried out at the ESAT Laboratory of KU Leuven, in the frame of (a) the FP7-PEOPLE Marie Curie Initial Training Network "Dereverberation and Reverberation of Audio, Music, and Speech (DREAMS)", funded by the European Commission under Grant Agreement no. 316969, (b) KU Leuven Research Council CoE PFV/10/002 (OPTEC), (c) KU Leuven Impulsfonds IMP/14/037 and was supported by (d) a Postdoctoral Fellowship (F+/14/045) of the KU Leuven Research Fund. The scientific responsibility is assumed by the authors.

The authors would like to thank Niccolò Antonello, Naveen Desiraju, Clement Doire, Christine Evers, Sina Hafezi, Mathieu Hu, Hamza Javed, Ante Jukić, Adam Kuklasinski, Alastair Moore, Pablo Peso, Richard Stanton, Giacomo Vairetti, and Costas Yiallourides, for helping carry out the experiment; Benjamin Cauchi, Clement Doire, and Mathieu Hu for helping set up the experiment; Ray Thompson for designing and building the structure

of the rotating platform; and all the subjects for taking part in the experiment.

5. REFERENCES

[1] J. Blauert, *Spatial Hearing: The Psychophysics of Human Sound Localization*. MIT Press, 1997.

[2] P. Strumillo, *Advances in Sound Localization*. InTech, 2011.

[3] D. R. Begault, E. M. Wenzel, and M. R. Anderson, "Direct comparison of the impact of head tracking, reverberation, and individualized head-related transfer functions on the spatial perception of a virtual speech source," *J. Audio Eng. Soc.*, vol. 49, no. 10, pp. 904–916, 2001.

[4] W. M. Hartmann, "Localization of sound in rooms," *J. Acoust. Soc. Am.*, vol. 74, no. 5, pp. 1380–1391, 1983.

[5] E. De Sena, H. Hacıhabiboğlu, and Z. Cvetković, "Analysis and design of multichannel systems for perceptual sound field reconstruction," *IEEE Trans. on Audio, Speech and Language Process.*, vol. 21, pp. 1653–1665, August 2013.

[6] Bang and Olufsen, "Music for archimedes." CD B&O 101, 1992.

[7] Various, *Standard 532b. Acoustics–Method for calculating loudness level*. ISO, 1975.

[8] B. R. Glasberg and B. C. Moore, "A model of loudness applicable to time-varying sounds," *J. Audio Eng. Soc.*, vol. 50, no. 5, pp. 331–342, 2002.

[9] B. Gardner and K. Martin, "Hrft measurements of a kemar dummy-head microphone," tech. rep., MIT Media Lab Perceptual Computing - Technical Report 280, May 1994.

[10] V. R. Algazi, R. O. Duda, D. M. Thompson, and C. Avendano, "The CIPIC hrtf database," in *IEEE Workshop on Appl. of Signal Process. to Audio and Acoust. (WASPAA-2001)*, pp. 99–102, IEEE, 2001.

[11] E. De Sena, H. Hacıhabiboğlu, Z. Cvetković, and J. Smith, "Efficient synthesis of room acoustics via scattering delay networks," *IEEE/ACM Trans. on Audio, Speech, and Language Process.*, vol. 23, pp. 1478–1492, Sept. 2015.

[12] J. B. Allen and D. A. Berkley, "Image method for efficiently simulating small-room acoustics," *J. Acoust. Soc. Am.*, vol. 65, no. 4, pp. 943–950, 1979.

[13] P. Huang and J. S. Abel, "Aspects of reverberation echo density." presented at the 123rd Audio Eng. Soc. Conv., Preprint #7163, New York, USA, Oct. 2007.

[14] Various, *Recomm. BS.1116-1, Methods for the Subjective Assessment of Small Impairments in Audio Systems including Multichannel Audio Systems*. ITU-R, 1997.

[15] E. De Sena, N. Antonello, M. Moonen, and T. van Waterschoot, "On the modeling of rectangular geometries in room acoustic simulations," *IEEE/ACM Trans. on Audio, Speech, and Language Process.*, vol. 23, pp. 774–786, Apr. 2015.

[16] S. Carlile, P. Leong, and S. Hyams, "The nature and distribution of errors in sound localization by human listeners," *Hearing research*, vol. 114, no. 1, pp. 179–196, 1997.

[17] T. R. Letowski and S. T. Letowski, "Auditory spatial perception: auditory localization," Tech. Rep. ARL-TR-6016, U.S. Army Research Laboratory, 2012.

[18] D. R. Begault, "Perceptual Effects of Synthetic Reverberationon Three- Dimensional Audio Systems," *J. Audio Eng. Soc.*, vol. 40, no. 11, pp. 895–904, 1992.

[19] S. Carlile, P. Leong, and S. Hyams, "The nature and distribution of errors in sound localization by human listeners," *Hearing Research*, vol. 114, no. 1-2, pp. 179–196, 1997.

[20] A. Dufour, P. Touzalin, and V. Candas, "Rightward shift of the auditory subjective straight ahead in right- and left-handed subjects," *Neuropsychologia*, vol. 45, no. 2, pp. 447–453, 2007.

[21] Y. Sosa, W. A. Teder-Sälejärvi, and M. E. McCourt, "Biases of spatial attention in vision and audition," *Brain and Cognition*, vol. 73, no. 3, pp. 229–235, 2010.

[22] [On-line]. Available: http://www.desena.org/sse.